ELSEVIER

Journal of Nuclear Materials 247 (1997) 208–214

journal of nuclear materials

Section 6. Metals and alloys

Pb–17Li and lithium: A thermodynamic rationalisation of their radically different chemistry

Peter Hubberstey *

Chemistry Department, Nottingham University, Nottingham, NG7 2RD, UK

Abstract

The contrasting chemistry of Pb–17Li and lithium is attributed to their lithium activities. Pb–Li alloys exhibit marked negative deviations from ideality owing to 'chemical short range order', giving $\gamma_{Li} = 7.26 \times 10^{-4}$, $a_{Li} = 1.23 \times 10^{-4}$ and $\overline{G}_{Li} = -57.8$ kJ mol^{-1} in Pb–17Li at 773 K. This $\overline{G}_{Li}$ value is sufficiently negative to prevent the reaction of Pb–17Li with gaseous hydrogen and nitrogen to form LiH and Li_3N but not with oxygen containing gases to form Li_2O. Similarly, nitride and carbide ceramics are compatible with Pb–17Li but oxide ceramics are liable to degradation. In contrast, unit activity liquid lithium reacts with all the gases and, depending on their free energy of formation, some of the ceramics. Wherea, dissolved oxygen is corrosive in Pb–17Li, giving $LiCrO_2$, dissolved nitrogen adopts the corrosive role in lithium giving Li_9CrN_5. The instability of LiH in Pb–17Li renders tritium extraction facile; this contrasts with lithium for which tritium extraction is difficult owing to LiH formation. © 1997 Elsevier Science B.V.

1. Introduction

Liquid lithium initially [1] and liquid Pb–17Li [2,3] more recently have been established as potential tritium breeder blanket materials for fusion energy systems. From an extensive series of fusion technology programs, huge databases have been accumulated for both candidates [4–6]. It quickly became apparent that chemical properties of the two liquids are quite different, lithium being generally much more reactive than Pb–17Li. In this paper, we report the results of a thermodynamic analysis of their radically different chemistry.

2. Pb–Li thermodynamics

Consideration of the Pb–Li phase diagram [7,8] shows that several intermetallic compounds exist in the composition range between lithium and Pb–17Li. These materials are quite stable as evidenced by their melting/decomposition temperatures and free energies of formation (Table 1). Their stabilities are indicative of low lithium and lead activities (a_{Li} and a_{Pb}), which are mirrored by large negative deviations from ideality (i.e., γ_{Li} and $\gamma_{Pb} \ll 1$) for the liquid alloys. This results in very low a_{Li} values for Pb–17Li. Several authors have studied the thermodynamics of the Pb–Li system. We have critically assessed their results and have derived a_{Li}, from which $\overline{G}_{Li}$ ($= RT \ln a_{Li}$) can be calculated, as a function of both composition and temperature. Owing to a discontinuity in the $a_{Li} - x_{Li}$ dependence close to Pb–17Li, the data have been calculated separately for lead-rich ($x_{Li} \leq 0.17$) [9] and lithium-rich ($x_{Li} \geq 0.17$) [10] systems. Where they overlap, the two sets of data correlate extremely well. Typically, the temperature ($1023 > T/K > 523$) dependence of a_{Li} for Pb–17Li and the composition dependence ($1.0 > x_{Li} > 0.1$) of a_{Li} at 773 K, calculated from the lithium-rich data, are given by the expressions:

$$\ln a_{Li} = -0.2882 - 6732/(T/K) \quad (1)$$

and

$$\ln a_{Li} = -10.724 + 11.211 \cdot x_{Li} - 7.329 \cdot x_{Li^2} + 6.841 \cdot x_{Li^3}. \quad (2)$$

Although activity data have been calculated throughout the composition ($1.0 > x_{Li} > 0.1$) and temperature ($1023 > T/K > 523$) ranges, they are only valid for the single (liquid) phase. In the two-phase regions, bounded by

* Corresponding author. Tel.: +44-115 951 3509; fax: +44-115 951 3563; e-mail: peter.hubberstey@nottingham.ac.uk.

0022-3115/97/$17.00
PII S0022-3115(97)00071-8

Table 1
Li_xPb_y phases; melting/decomposition temperatures and free energies of formation

Phase	x_{Li}	M.Pt. (K)	$\Delta_f G°$ (kJ mol^{-1})
LiPb	0.500	755 [a]	−60
Li_8Pb_3	0.727	915 [b]	−377
Li_3Pb	0.750	931 [b]	−137
Li_7Pb_2	0.778	999 [a]	−316
$Li_{22}Pb_5$	0.815	923 [b]	−791

[a] Congruently melting.
[b] Peritectically decomposing.

(liquid + LiPb) and (liquid + $Li_{22}Pb_5$) (see Fig. 2 for a schematical representation of the pertinent section of the phase diagram), they are not strictly applicable; nonetheless, their magnitude can be used to assess the variation in the chemistry of the Pb–Li alloys.

3. Thermodynamics of dissolved solutes in Pb–Li alloys

The activities of dissolved solutes, particularly oxygen, hydrogen, nitrogen and carbon, can be calculated for saturated solutions under equilibrium conditions from reactions typified by:

$$2Li(Pb\text{–}Li) + O(Pb\text{–}Li) \overset{\Delta_f G°(Li_2O,\,c,\,T/K)}{\rightleftharpoons} Li_2O(c). \quad (3)$$

Hence

$$\Delta_f G°(Li_2O) = RT \ln K_e = RT \ln\left\{a_{Li_2O}/a_{Li}^2 \cdot a_O\right\} \quad (4)$$

or

$$\ln a_O = \left\{-\Delta_f G°(Li_2O)/RT\right\} - 2 \ln a_{Li}. \quad (5)$$

Activity data for the four non-metal solutes were calculated using standard free energy of formation data [11,12] and the lithium activity data quoted above. The results at 773 K are depicted in Fig. 1 as $\ln a_X$ against x_{Li} plots, together with $\ln a_{Li}$ data. Solute activity generally increases ($\ln a_X$ becomes more positive) as lithium activity decreases ($\ln a_{Li}$ becomes less positive). Oxygen activity is low ($\ln a_O$ is large and negative) throughout the composition range. Hydrogen, nitrogen and carbon activities, however, are much greater and increase above unity ($\ln a_X$ changes from negative to positive values) with decreasing x_{Li}. Hence, at low x_{Li}, LiH, Li_3N and Li_2C_2 are not stable, but decompose to give non-metal in its standard state and dissolved lithium. The driving forces for this process are the increasingly negative partial free energy of dissolved lithium ($\overline{G}_{Li} = RT \ln a_{Li}$) and the relatively low free energies of formation of LiH, Li_3N and Li_2C_2 [11,12]. To stabilise, for example, LiH in Pb–17Li at 773 K, would require a hydrogen overpressure of $\simeq 650$ MPa. This result is of immense significance in interpreting the radically different chemistries of lithium and Pb–17Li.

4. Reaction with atmospheric contaminants

If the reaction of nitrogen with Pb–Li alloys to produce Li_3N

$$3Li(Pb\text{–}Li) + 0.5N_2(g) \overset{\text{liquid Pb–Li alloy}}{\rightarrow} Li_3N(c) \quad (6)$$

is taken as an example, then

$$\Delta_r G° = \Delta_f G°(Li_3N,\,c,\,T/K) - \left\{3RT \ln a_{Li} + 0.5RT \ln a_{N_2}\right\} = \Delta_f G°(Li_3N,\,c,\,T/K) - \left\{3\overline{G}_{Li} + 0.5RT \ln p_{N_2}/p^*_{N_2}\right\}. \quad (7)$$

Standard free energy of formation data were taken from critically assessed NBS compilations [11,12], $\overline{G}_{Li}$ data

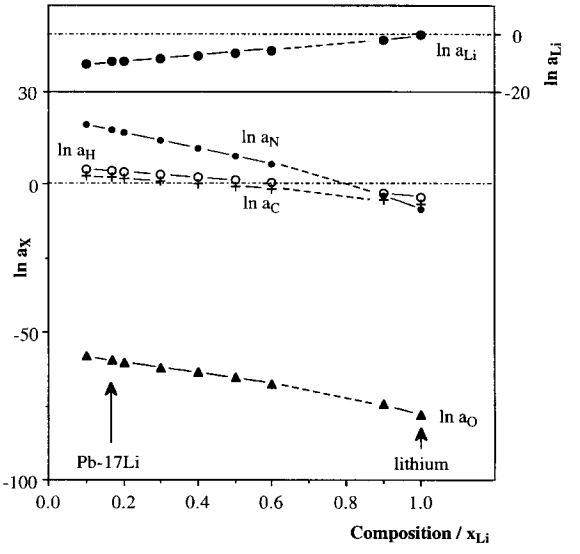

Fig. 1. Activity-composition relationships for saturated solutions of oxygen, nitrogen, hydrogen and carbon, together with that for lithium, in Pb–Li alloys at 773 K.

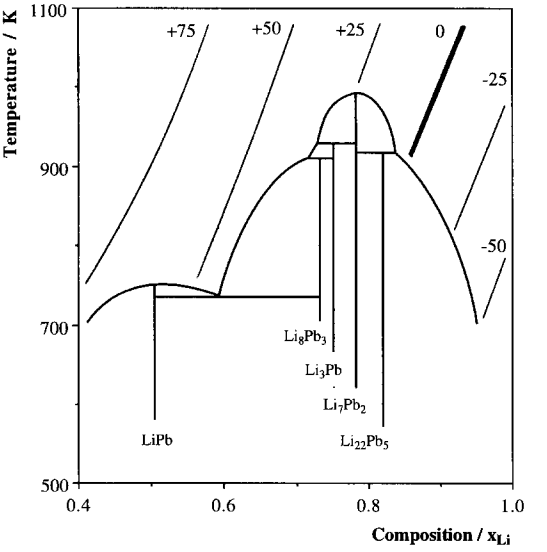

Fig. 2. $\Delta_r G°$ (kJ (mol Li_3N)$^{-1}$) data for the reaction of Pb–Li alloys with nitrogen gas ($p_{N2}/p^*_{N2} = 0.781$) to form Li_3N. (The values given against the curves represent their free energy).

from the calculated a_{Li} data and p_{N2}/p^*_{N2} was assumed to be 0.781 (as in air).

$\Delta_r G^\circ$ data were generated in the form of 2D temperature-composition matrices. They are presented diagrammatically in Fig. 2, as lines of constant free energy on temperature (ordinate) and composition (abscissa) axes. Fig. 2 also contains a schematic representation of the pertinent section of the Pb–Li phase diagram to show the parameter ranges under which the calculations are valid. $\Delta_r G^\circ$ becomes more positive with decreasing composition and increasing temperature. As indicated in Section 3, reaction only occurs ($\Delta_r G^\circ$ is negative) at high x_{Li}, the reaction limit being represented by the bold line for which $\Delta_r G^\circ = 0$.

Similar calculations have been completed for reaction with oxygen ($p_{O2}/p^*_{O2} = 0.210$ as in air), hydrogen ($p_{H2}/p^*_{H2} = 1$) and carbon. The data mirror the $\ln a_X$ against x_{Li} data (Section 3). Although for reaction with oxygen, $\Delta_r G^\circ$ is negative throughout; for hydrogen and carbon it changes from negative to positive with decreasing x_{Li}. The results are summarised in Fig. 3, which shows the temperature and composition dependence of the reaction limit ($\Delta_r G^\circ = 0$) for Li_3N, LiH and Li_2C_2 formation. The calculations thus rationalise the experimental observation that whereas lithium reacts with all four non-metals to form salts, Pb–17Li only reacts with oxygen to form Li_2O.

The low activity (large, negative $\overline{G}_O$) of dissolved oxygen in Pb–Li alloys, can be used to rationalise the observed reduction of H_2O [9], CO [13] and CO_2 [13]. $\Delta_r G^\circ$ values calculated using expressions similar to Eqs. (6) and (7), assuming the pressure of the gaseous reactant

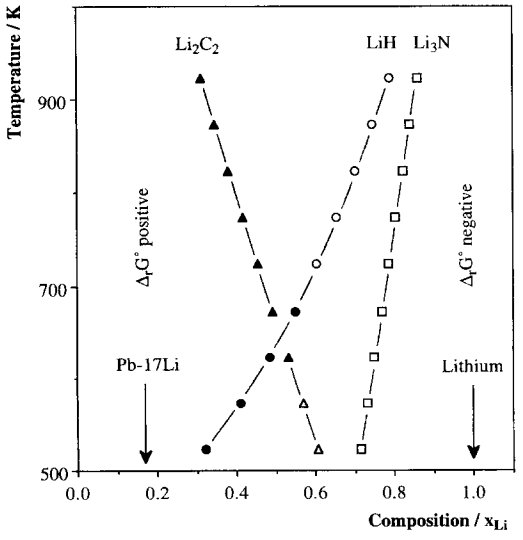

Fig. 3. Limit of formation ($\Delta_r G^\circ = 0$) of Li_3N (from N_2 gas ($p_{N2}/p^*_{N2} = 0.781$)), LiH (from H_2 gas ($p_{H2}/p^*_{H2} = 1$)) and Li_2C_2 (from carbon) in Pb–Li alloys at 773 K.

Table 2
Gibbs energies of reaction ($\Delta_r G^\circ$) of gas phase H_2O, CO and CO_2 (partial pressure = 0.001 MPa) with Pb–17Li and lithium at 773 K

Reaction	$\Delta_r G^\circ$ (kJ mol^{-1})		
	Pb17Li	lithium	
	O satd.	O. satd.	473 K CT
H_2O [a]	−148	−323	−414
CO [b]	−172	−332	−397
CO_2 [b]	−338	−614	−714

[a] Reaction products Li_2O and H_2 (for Pb–17Li) or LiH (for lithium).
[b] Reaction products Li_2O and C (for Pb–17Li) or Li_2C_2 (for lithium).

to be 0.001 MPa (1 mol% of the atmosphere), are negative throughout. Typical values at 773 K are given in Table 2.

5. Non-metal solubilities and tritium release

The ramifications of the activity data discussed in Section 3 are immense. Although salts precipitate from solutions of all four non-metals in liquid lithium, only Li_2O precipitates from Pb–17Li. Solubility data for the four lithium systems (Table 3) are well established [14] in the form

$$\ln x_X = A + B/T(\mathrm{K}).$$

The solubility of oxygen in Pb–17Li is under discussion, owing to its extremely small magnitude; it is thought to be less than 3×10^{-3} wppm ($x_O = 3.25 \times 10^{-8}$) at 743 K or 1×10^{-2} wppm ($x_O = 1.08 \times 10^{-7}$) at 823 K [15]. These values can be compared to those of oxygen in lead ($x_O = 3.14 \times 10^{-5}$ at 743 K [16]) and lithium ($x_O = 5.34 \times 10^{-4}$ at 743 K [14]). They are so low that, under normal breeder blanket operating conditions, crystalline Li_2O can be assumed to be present in equilibrium with oxygen saturated Pb–17Li.

The solubilities (x_X) of hydrogen and nitrogen in liquid Pb–17Li vary with their partial pressure (p) according to Sieverts' law:

$$x_X = K_s p^{0.5}.$$

Although data are not available for nitrogen solutions, hydrogen solutions have been extensively investigated as part of tritium release studies. For these solutions [4–6], the temperature dependence of Sieverts constant is given by the expression:

$$K_s = 2.44 \times 10^{-8} \exp(-1350/RT) \text{ units: at. frac. Pa}^{-0.5}.$$

The amount of hydrogen (tritium) or nitrogen found in Pb–17Li is thus determined by its partial pressure; de-

creasing partial pressure will result in decreasing inventories. Hence, tritium release from Pb–17Li is a chemically facile process and under normal operating conditions the amount of tritium in the breeder blanket will be extremely low.

Solute activities in saturated solutions under equilibrium conditions can be calculated, since the free energy change for the typical reaction

$$2\mathrm{Li(Pb\text{–}Li)} + \mathrm{O(Pb\text{–}Li)} \rightarrow \mathrm{Li_2O(c)}. \quad (8)$$

is zero. Hence

$$RT \ln a_O = \overline{G}_O(\mathrm{Pb\text{–}Li}) = \Delta_f G^\circ(\mathrm{Li_2O}) - 2\overline{G}_{Li}(\mathrm{Pb\text{–}Li}). \quad (9)$$

However, the magnitude and temperature dependence of non-metal solubilities in liquid lithium are such that unsaturated solutions can be generated by various methods including cold trapping. Dilution generates reduced activities and more negative $\overline{G}_X$ values:

$$RT \ln a_O = \Delta_f G^\circ(\mathrm{Li_2O}) - 2\overline{G}_{Li}(\mathrm{Pb\text{–}Li}) + RT \ln x_O/x_O^*, \quad (10)$$

where x_O is the mole fraction of oxygen present in the solution and x_O^* is the value at saturation. For liquid lithium, $a_{Li} = 1$, and Eq. (10) reduces to

$$RT \ln a_O = \Delta_f G^\circ(\mathrm{Li_2O}) + RT \ln x_O/x_O^*. \quad (11)$$

$\overline{G}_X$ (X = O, H, N and C) data for saturated and unsaturated (cold trapped at 473 and 573 K) lithium (obtained using Eq. (11)) are collated in Table 3. The $\overline{G}_X$ values become more negative (i.e., the solutions become more stable) as the solution concentration is decreased. Hence, tritium release from lithium becomes progressively more difficult as its concentration decreases. This poses a major problem in the application of lithium as tritium breeder.

6. Compatibility with ceramic coating materials

Oxides, (Al_2O_3, Cr_2O_3, Y_2O_3, CaO and MgO), nitrides (AlN, TiN) and carbides (β-SiC, TiC) are presently being considered for application as ceramic coatings for Pb–17Li tritium breeder blanket containment materials to address the critical issues of magnetohydrodynamic pressure drops, high temperature corrosion and tritium loss [17–23].

The chemical viability of a ceramic in liquid Pb–Li alloys is given by the free energy change ($\Delta_r G^\circ$) of the typical reaction

$$\mathrm{Y_2O_3(c)} \xrightarrow{\text{liquid Pb–Li alloy}} 3\mathrm{O(Pb\text{–}Li)} + 2\mathrm{Y(c)}, \quad (12)$$

$$\Delta_r G^\circ = (1/2)\{3\overline{G}_O(\mathrm{Pb\text{–}Li}) - \Delta_f G^\circ(\mathrm{Y_2O_3})\} \quad (13)$$

(the reduced metal is assumed to be at unit activity). Introducing Eq. (10) gives

$$\Delta_r G^\circ = (1/2)\{3[\Delta_f G^\circ(\mathrm{Li_2O}) - 2\overline{G}_{Li}(\mathrm{Pb\text{–}Li}) + RT \ln x_O/x_O^*] - \Delta_f G^\circ(\mathrm{Y_2O_3})\}. \quad (14)$$

$\Delta_r G^\circ$ has been calculated for the degradation of diverse binary oxides, nitrides and carbides as a function of tem-

Table 3
Solubility data {$\ln x_X = A + B/T$} and derived $\overline{G}_X$ data for non-metals in liquid lithium

	A	B	T (K)				
Oxygen	1.428	−6659	530–715				
Hydrogen	3.507	−5314	523–775				
Nitrogen	2.976	−4832	468–723				
Carbon	−1.1	−5750	477–908				
		$\overline{G}_X$ (kJ mol X^{-1})					
Temperature (K)		573	673	773	873	973	
Oxygen	satd.	−524.9	−511.1	−497.3	−483.5	−469.7	
	573 K	−524.9	−520.8	−516.6	−512.5	−508.4	
	473 K	−536.6	−534.5	−532.4	−530.3	−528.2	
Hydrogen	satd.	−46.2	−37.9	−29.6	−21.3	−13.1	
	573 K	−46.2	−45.6	−45.0	−44.5	−43.9	
	473 K	−55.5	−56.6	−57.6	−58.7	−59.8	
Nitrogen	satd.	−84.0	−70.1	−56.2	−42.3	−28.4	
	573 K	−84.0	−77.1	−70.2	−63.3	−56.4	
	473 K	−92.5	−87.0	−81.6	−76.2	−70.8	
Carbon	satd.	−38.4	−41.0	−44.0	−47.4	−51.2	
	573 K	−38.4	−49.3	−60.7	−72.4	−84.5	
	473 K	−48.5	−61.2	−74.3	−87.8	−101.7	

473 K cold trapped lithium contains $x_O = 3.21 \times 10^{-6}$, $x_H = 4.05 \times 10^{-4}$, $x_N = 7.17 \times 10^{-4}$, $x_C = 1.75 \times 10^{-6}$; 573 K cold trapped lithium contains $x_O = 3.74 \times 10^{-5}$, $x_H = 3.13 \times 10^{-3}$, $x_N = 4.27 \times 10^{-3}$, $x_C = 1.46 \times 10^{-5}$ [14].

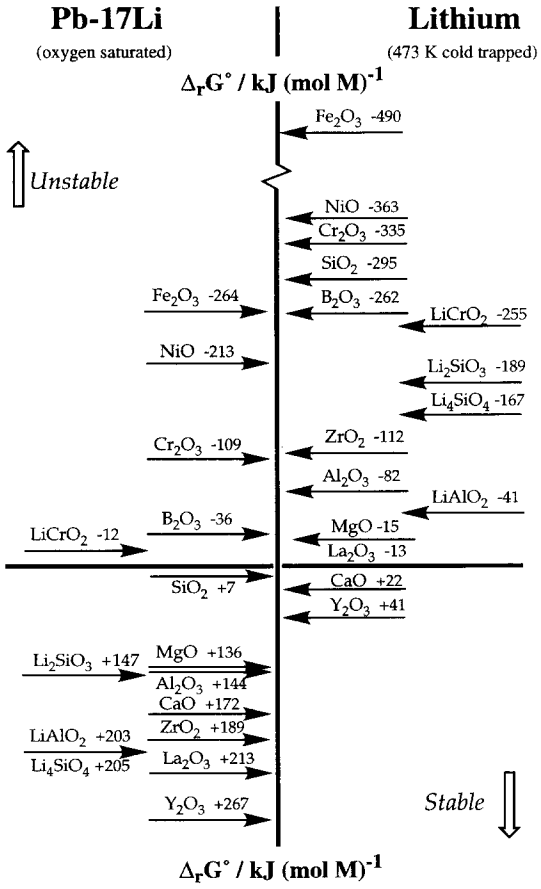

Fig. 4. $\Delta_r G^\circ$ (kJ (mol M)$^{-1}$) data for the reaction at 773 K of various oxide ceramics with oxygen saturated Pb–17Li and with 473 K cold trapped lithium ($x_O = 3.21 \times 10^{-6}$).

perature and composition (x_{Li}). Since ternary oxide formation has been observed in both breeder materials by several authors ($LiCrO_2$ [24,25] and $LiYO_2$ [26]) and has been shown to be thermodynamically favourable [27], their degradation has also been considered. The results have been discussed in detail elsewhere [10,27].

The $\Delta_r G^\circ$ values for the nitride (MN (M = B, Al, Ti, Zr, V, Ta, and Cr) and Si_3N_4) and carbide (MC (M = β-Si, Ti, Zr, Nb, Ta)) ceramics are generally positive. They are more positive in non-metal saturated Pb–Li alloys than in 473 K cold trapped lithium, indicating a greater stability towards the former. The only ceramics found to be unstable were Si_3N_4, β-SiC and CrN in 473 K cold trapped lithium ($\Delta_r G^\circ = -14$, -1 and -20 kJ (mol metal)$^{-1}$, respectively, at 773 K).

The calculations predict much more variable behaviour for the oxides. $\Delta_r G^\circ$ values at 773 K are compared schematically in Fig. 4; they are directly comparable as they are given per mole of metal. Although the majority are stable in oxygen saturated Pb–17Li, Fe_2O_3, NiO, Cr_2O_3, B_2O_3 and $LiCrO_2$ reduce to the metal and SiO_2 has $\Delta_r G^\circ \simeq 0$. There is a greater tendency to decomposition in 473 K cold trapped lithium, the only oxides predicted to be stable being Y_2O_3, Sc_2O_3 (not included on Fig. 4; $\Delta_r G^\circ = +41$ kJ (mol metal)$^{-1}$ at 773K) and CaO. It is important to note that the ternary oxides are intrinsically more stable to reduction to the metal than the binary oxides, their stabilities increasing with increasing Li_2O content (e.g., from Li_2SiO_3 to Li_4SiO_4) (Fig. 4). This observation is consistent with the fact that conversion of binary to ternary compounds is favourable [27], a feature which must be remembered when considering both the stability of ceramics and corrosion processes (Section 7) in these liquid breeder materials. Hence, although Y_2O_3 and Sc_2O_3 are stable to reduction, they may undergo conversion to $LiYO_2$ and $LiScO_2$ as noted for $LiYO_2$ in lithium [26].

This analysis assumes that the reduced metals are generated at unit activity. Although this is a realistic assumption for the majority, aluminium and silicon are highly soluble in liquid lithium [7,8] and so will have markedly reduced activities. This will have the effect of further destabilising the ceramic.

7. Corrosion chemistry

The corrosion of containment materials by lithium and by Pb–17Li is a fundamental problem. In both solvents, it is thought that corrosion proceeds primarily via a dissolution (loss of nickel and manganese to give a ferritic zone) rather than a chemical process, although Li_9CrN_5 [28] and $LiCrO_2$ [24,25] occur on steels exposed to lithium and Pb–17Li, respectively. The thermodynamic analysis is consistent with these observations. Consideration of Fig. 4 shows that the binary oxides of the principal components of steels (Fe, Ni, Cr) are unstable in both liquids, suggesting that none would be formed in corrosion processes. However, $\Delta_r G^\circ$ for the reduction of the ternary oxide $LiCrO_2$ is very small and it might be a possible corrosion product. Similarly small positive $\Delta_r G^\circ$ values occur for the nitride, CrN and the carbides, $Cr_{23}C_6$, Cr_7C_3 and Cr_3C_2.

In view of these points, the analysis for this section has been restricted to the formation of chromium compounds. $\Delta_r G^\circ$ for the typical corrosion process

$$Cr(steel) + N(Li) \rightarrow CrN(c) \qquad (15)$$

is given by the expression

$$\Delta_r G'' = \Delta_f G^\circ(CrN, c, T/K) - \left(\overline{G}_{Cr} + \overline{G}_N\right). \qquad (16)$$

Standard free energy of formation data were taken from critically assessed NBS compilations [11,12], free energy data for chromium ($\overline{G}_{Cr}$) were derived from the activity data ($\log a_{Cr} = -0.613 + 54.95/T(K)$) reported by Gnanamoorthy for AISI 316LN SS [29] and non-metal free

energies ($\overline{G}_N$) were calculated using Eq. (10). $\Delta_r G^\circ$ values for the formation of Cr_2O_3, $LiCrO_2$, Cr_3C_2, CrN and $Cr_{23}C_6$ in 473 K cold trapped lithium are compared in Fig. 5. Although there is no possibility of oxide formation, nitride and carbide formation is only just positive. Increasing the nitrogen or carbon activity (by increasing the cold trap temperature) will result in more negative $\Delta_r G^\circ$ values and the formation of nitride and carbide corrosion products. Although thermodynamic data are not available for ternary nitrides, if it is assumed that the formation of ternary from binary nitrides is as favourable as for oxides, the formation of ternary nitrides is a real possibility. Using very preliminary data for $\Delta_f G^\circ$ (Li_9CrN_5, c, 750 K) = -525 kJ mol^{-1} [30] the formation of Li_9CrN_5 in lithium systems is plausible ($\Delta_r G^\circ = -79$ kJ mol^{-1} at 750 K). This data point is included in Fig. 5.

Nitrogen is the corrosive solute in lithium, adopting the role of oxygen in sodium. As well as Li_9CrN_5, the formation of Li_7VN_4, Li_3FeN_2, Li_5SiN_3 and Li_2NCN has been noted in liquid lithium.

The situation is quite different in Pb–17Li as Li_2O is the only salt stable in this medium. $\Delta_r G^\circ$ values for oxide formation in Pb–17Li are compared to those in 473 K cold trapped lithium in Fig. 6. Two significant points arise. First, the formation of the oxides is more favourable in oxygen saturated Pb–17Li and, second, the formation of $LiCrO_2$ is more favourable than that of Cr_2O_3. The $\Delta_r G^\circ$ values for formation of $LiCrO_2$ on 316 SS immersed in oxygen saturated Pb–17Li is only just positive (= 20 kJ mol^{-1} at 773 K (Fig. 6)). These data are particularly sensitive to $\overline{G}_{Li}$; an error of 7 kJ mol^{-1} in the latter would be sufficient to give a negative $\Delta_r G^\circ$ value consistent with the observations [24,25].

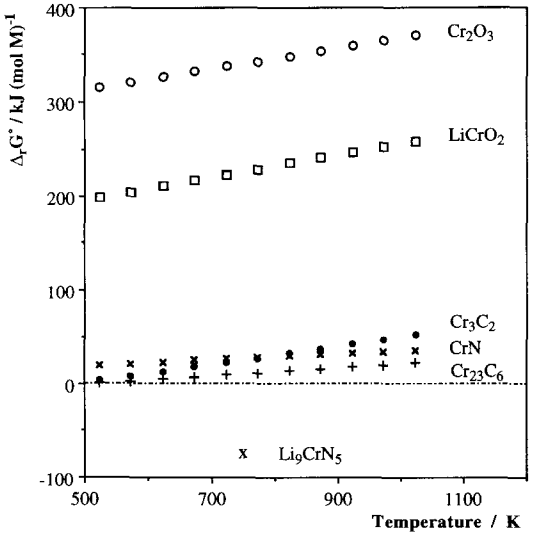

Fig. 5. Temperature dependence of the free energy of formation, $\Delta_r G^\circ$ (kJ mol M^{-1}), of potential chromium-containing corrosion products in 473 K cold trapped lithium ($x_O = 3.21 \times 10^{-6}$; $x_N = 7.17 \times 10^{-4}$; $x_C = 1.75 \times 10^{-6}$).

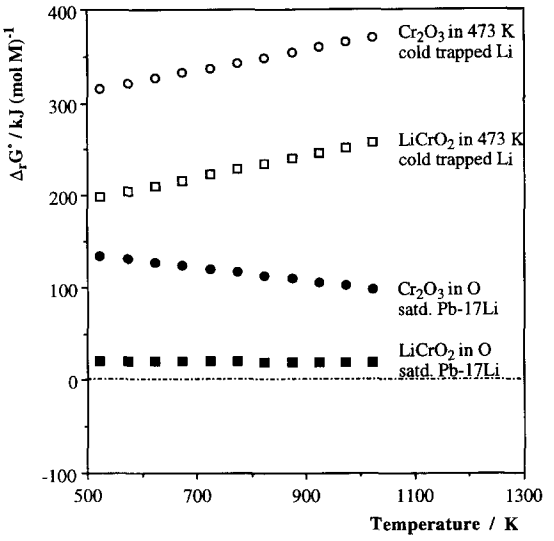

Fig. 6. Temperature dependence of the free energy of formation, $\Delta_r G^\circ$ (kJ mol M^{-1}), of Cr_2O_3 and $LiCrO_2$ in oxygen saturated Pb–17Li and in 473 K cold trapped lithium ($x_O = 3.21 \times 10^{-6}$).

8. Conclusions

The chemical differences between Pb–17Li and lithium are due to their different lithium activities. Pb–Li alloys exhibit marked negative deviations from ideality owing to 'chemical short range order' [31], giving Pb–17Li $\gamma_{Li} = 7.26 \times 10^{-4}$, $a_{Li} = 1.23 \times 10^{-4}$ and $\overline{G}_{Li} = -57.8$ kJ mol^{-1} at 773 K. These values are such that LiH, Li_3N and Li_2C_2, which have low thermodynamic stabilities, cannot co-exist with Pb–17Li. Hence although gaseous hydrogen, nitrogen and oxygen react with liquid lithium to form the corresponding salt, only oxygen (and oxygen containing gases; H_2O, CO, CO_2) will react with Pb–17Li to form crystalline Li_2O. The instability of LiH in Pb–17Li renders tritium extraction facile; this contrasts with lithium for which tritium extraction is difficult owing to LiH formation.

Nitrogen is the corrosive solute in lithium, forming Li_9CrN_5 on steel surfaces. Chemical corrosion is limited in Pb–17Li, Li_3N and Li_2C_2 being unstable, but there is some evidence for $LiCrO_2$ formation. In both liquids, corrosion primarily proceeds via a dissolution-deposition process (involving Ni and Mn).

All carbides and nitrides are compatible with Pb–17Li; with the exception of β-SiC, Si_3N_4 and CrN, they are also stable in unsaturated lithium. In contrast, some oxides are reduced to the metal in Pb–17Li and, with the exception of Y_2O_3, Sc_2O_3 and CaO all are incompatible with unsaturated lithium.

References

[1] H.U. Borgstedt, C.K. Mathews, Applied Chemistry of the Alkali Metals (Plenum, New York, 1987).
[2] G. Casini, Ph. Labbe, M. Reiger, L. Baraev, M. Biggio, F. Farfaletti-Casali, G. Gervaise, L. Giancarli, M. Roze, Y. Severi, J. Quintrec-Bossy, S. Tomminetti, J. Wu, M. Zucchetti, Fusion Eng. Des. 14 (1991) 353.
[3] V. Coen, T. Sample, Fusion Technol. 1 (1990) 248.
[4] D.L. Smith, G.D. Morgan, USDOE Report ANL/FPP-84-1, Vol. 2, 1984, p. 6-1.
[5] M. Küchle, KfK Report Material Database for the NET Test Blanket Design Studies, Feb. 1990.
[6] B. Schulz, Fusion Eng. Des. 14 (1991) 273.
[7] A.D. Moffatt, Moffatt's Handbook of Binary Phase Diagrams 1992.
[8] T.B. Massalski, Binary Alloy Phase Diagrams (ASM International, Materials Park, OH, 1990).
[9] P. Hubberstey, T. Sample, J. Nucl. Mater. 199 (1993) 149.
[10] P. Hubberstey, T. Sample, Proc. Int. Conf. Interfacial Effects in Quantum Engineering Systems, Mito, 21–23 Aug. 1996, J. Nucl. Mater., to be published.
[11] M.W. Chase, C.A. Davis, J.R. Downey, D.J. Frurip, R.A. McDonald, A.N. Syverud, J. Phys. Chem. Ref. Data 14 (1) (1985).
[12] C.E. Wicks and F.E.Block, US Bureau of Mines Bulletin, Vol. 606, 1963
[13] P. Hubberstey, T. Sample, J. Nucl. Mater. 191–194 (1992) 277.
[14] P. Hubberstey, A.T. Dadd, P.G. Roberts, in: Liquid Metal Systems, Vol. 445, ed. H.U. Borgstedt (Plenum, New York, 1982).
[15] M.G. Barker, J.A. Lees, T. Sample, Proc. 4th. Int. Conf. Liquid Metal Eng. and Technol., Avignon, Vol. 1, Paper 206, 1984.
[16] C.B. Alcock, T.N. Belford, Trans. Faraday Soc. 60 (1964) 822.
[17] A. Perujo, K. Forcey, Fusion Eng. Design 28 (1995) 252.
[18] H. Glasbrenner, A. Perujo, E. Senna, Fusion Technol. 28 (1995) 1159.
[19] H.U. Borgstedt, H. Glasbrenner, Z. Peric, J. Nucl. Mater. 212–215 (1994) 1501.
[20] H. Glasbrenner, H.U. Borgstedt, J. Nucl. Mater. 212–215 (1994) 1561.
[21] A. Terlain, T. Flament, J. Sannier, J.L. Raoault, Fusion Technol. 1 (1990) 916.
[22] I. Schreinlechner, P. Sattler, J. Nucl. Mater. 191–194 (1992) 970.
[23] V. Coen, H. Kolbe, L. Orecchia, M. Della Rossa, in: High Temperature Corrosion of Technical Ceramics (Elsevier, Amsterdam, 1989).
[24] M.G. Barker, V. Coen, H. Kolbe, J.A. Lees, L. Orecchia, T. Sample, J. Nucl. Mater. 155–157 (1988) 732.
[25] T. Sample, V. Coen, H. Kolbe, L. Orecchia, J. Nucl. Mater. 191–194 (1992) 979.
[26] T. Terai, European Workshop on Lithium and Pb–17Li Corrosion and Chemistry, Nottingham, 1995, personal communication.
[27] P. Hubberstey, T. Sample, A. Terlain, Fusion Technol. 28 (1995) 1194.
[28] M.G. Barker, P. Hubberstey, A.T. Dadd, S.A. Frankham, J. Nucl. Mater. 114 (1983) 143.
[29] A.M. Azad, O.M. Sreedharan, J.B. Gnanamoorthy, J. Nucl. Mater. 167 (1989) 82.
[30] P. Hubberstey, Proc. Int. Conf. Liquid Metal Engineering and Technology, Vol. 3, BNES, London, 1984, p. 85.
[31] H. Ruppersberg, H. Eggar, J. Chem. Phys. 63 (1975) 4095.